Preprint version accepted to appear in European Heart Journal Cardiovascular Imaging.
Final version of this paper available at https://academic.oup.com/ehjcimaging

3D right ventricular shape and strain in congenital heart disease patients with right ventricular chronic volume loading

Pamela Moceri * [a,b,c]; Nicolas Duchateau [d]; Stéphane Gillon[b]; Lolita Jaunay[b]; Delphine Baudouy [b]; Fabien Squara [b]; Emile Ferrari [b]; Maxime Sermesant[a].

Short title: 3D RV shape and strain in CHD with chronic volume loading

Manuscript total word count: 5657

[a] Université Côte d'Azur, Inria Epione team, Sophia Antipolis, France.
[b] Centre Hospitalier Universitaire de Nice, Service de Cardiologie, Nice, France.
[c] UR2CA, Université Côte d'Azur, Nice, France.
[d] Creatis, CNRS UMR5220, INSERM U1206, Université Lyon 1, France.

* Corresponding author: Dr Pamela Moceri, CHU de Nice – Hôpital Pasteur
Avenue de la voie romaine, CS 51069 – 06001 Nice, France.
Tel: +33 492037733 / Fax: +33 492038516
Email: moceri.p@chu-nice.fr

Preprint version accepted to appear in European Heart Journal Cardiovascular Imaging.
Final version of this paper available at https://academic.oup.com/ehjcimaging

ABSTRACT

Background: Right ventricular (RV) function assessment is crucial in congenital heart disease (CHD) patients, especially in atrial septal defect (ASD) and repaired Tetralogy of Fallot (TOF) patients with pulmonary regurgitation (PR). In this study, we aimed to analyse both 3D RV shape and deformation to better characterize RV function in ASD and TOF-PR.

Methods: We prospectively included 110 patients (≥16 years old) into this case-control study: 27 ASD patients, 28 with TOF and 55 sex- and age-matched healthy controls. Endocardial tracking was performed on 3D transthoracic RV echocardiographic sequences and output RV meshes were post-processed to extract local curvature and deformation. Differences in shape and deformation patterns between subgroups were quantified both globally and locally.

Results: Curvature highlights differences in RV shape between controls and patients while ASD and TOF-PR patients are similar. Conversely, strain highlights differences between controls and TOF-PR patients while ASD and controls are similar (global area strain: -31.5±5.8% [controls], -34.1±7.9% [ASD], -24.8±5.7% [TOF-PR], $p<0.001$, similar significance for longitudinal and circumferential strain). The regional and local analysis highlighted differences in particular in the RV free wall and the apical septum.

Conclusion: Chronic RV volume loading results in similar RV shape remodeling in both ASD and TOF patients while strain analysis

Preprint version accepted to appear in European Heart Journal Cardiovascular Imaging.
Final version of this paper available at https://academic.oup.com/ehjcimaging

demonstrated that RV strain is only reduced in the TOF group. This suggests a fundamentally different RV remodeling process between both conditions.

KEY-WORDS: Congenital heart disease; 3D echocardiography; Right ventricular function; Right ventricular strain; Curvature.

Preprint version accepted to appear in European Heart Journal Cardiovascular Imaging.
Final version of this paper available at https://academic.oup.com/ehjcimaging

INTRODUCTION

Right ventricular (RV) function evaluation is of utmost importance in congenital heart diseases (CHD)[1]. RV chronic volume loading is frequently observed in CHD and leads to right ventricular (RV) remodelling in terms of shape and function[2], which affects the patients' prognosis and in particular CHD patients[3].

RV response to pre- and after-load changes is a crucial issue in CHD. Atrial septal defect (ASD) with left to right shunting is generally well tolerated for years, while repaired tetralogy of Fallot (TOF) patients with chronic pulmonary regurgitation are at risk for developing RV dilatation and ultimately failure[4, 5].

The assessment of RV differences in shape and deformation is challenging given the peculiar RV geometry, which requires 3D imaging and dedicated analysis tools. The echocardiographic literature only focused on 2D regional and global observations on these populations. Local 3D descriptors such as curvature and strain have been recently exploited in the context of specific diseases affecting the RV (pulmonary hypertension, patients with left ventricular assist devices), but not in the context of RV chronic volume loading. In addition, they have only been examined separately, which may be limited when both shape and function are altered.

In this study, we investigated the effects of RV volume chronic volume loading on 3D descriptors of the RV anatomy and mechanics, both in ASD and TOF patients compared to a control group. We hypothesized

Preprint version accepted to appear in European Heart Journal Cardiovascular Imaging.
Final version of this paper available at https://academic.oup.com/ehjcimaging

that a finer analysis that integrates RV shape and deformation, in 3D and both globally and locally up to each point of the RV endocardial surface, could provide novel insights into the relationship between shape and function to better characterize these patients.

METHODS

Study design and patients

We performed a case control study on patients (adults and adolescents > 16 years old) with ASD and TOF with chronic pulmonary regurgitation followed up at the Pasteur University Hospital, Nice, FR between September 2016 and January 2019. Stable patients (no hospitalization during the 2 years preceding the inclusion) were enrolled into a standardized echocardiographic protocol including 2D and 3D echocardiography. Our study protocol was approved by the local research Ethics committee. Personal patient and parental or guardian's consent were obtained together with the adolescent's assent in patients < 18 years old.

Asymptomatic healthy volunteers (with no prior history of cardiovascular disease) were recruited from the community to serve as controls and were included if they had a normal transthoracic echocardiography, and if they were in sinus rhythm. They were matched 1/1 to the study population regarding age and sex.

ASD patients were included if they had no other defect and an open and significant left-to-right shunt at the atrial level with hemodynamic

Preprint version accepted to appear in European Heart Journal Cardiovascular Imaging.
Final version of this paper available at https://academic.oup.com/ehjcimaging

consequence defined by a basal RV diameter > 41mm[8]. ASD patients were excluded if they had pulmonary hypertension defined by mean pulmonary artery pressure ≥ 25mmHg and pulmonary vascular resistance > 3 Wood Units (assessed by right heart catheterization either during the initial assessment of a dilated right heart to eliminate pulmonary hypertension, or before the ASD closure procedure).

Repaired TOF patients were included if they had no other defect. Patients with significant residual pulmonary stenosis were excluded (maximum gradient across the pulmonary valve > 40mmHg). The presence of significant pulmonary regurgitation (at least moderate) was defined by a pulmonary regurgitation jet width on colour Doppler > 50% of the pulmonary annulus, a pulmonary regurgitation index < 0.77 (pulmonary regurgitation duration/diastolic duration ratio) and/or diastolic flow Doppler reversal[9-11].

Demographics and clinical data (age, gender, diagnosis, baseline WHO class, type of repair, number of surgeries) were collected at inclusion.

2D-echocardiographic acquisitions and measurements

Echocardiographic examinations were performed using an EPIQ-7 ultrasound system and an X5-1 transducer (Philips Medical system, Andover, MA, USA). Doppler echocardiography was performed per the recommendations of the American Society of Echocardiography and the European Association for Cardiovascular Imaging[12-14]. A cardiologist, with

Preprint version accepted to appear in European Heart Journal Cardiovascular Imaging.
Final version of this paper available at https://academic.oup.com/ehjcimaging

advanced training in echocardiography, performed the cine-loop acquisitions and interpreted the 2D datasets. The measured parameters were averaged over three consecutive cycles, and consisted of: left ventricular ejection fraction, right atrial area, tricuspid annular peak systolic velocity (s'), tricuspid annular plane systolic excursion (TAPSE), RV basal diameter and RV wall thickness.

3D transthoracic echocardiography

At least four 3D cine-loops were acquired from an apical 4-chamber view focused on the RV, using an IE-33 or EPIQ-7 ultrasound system and a matrix-array X5-1 transducer (Philips Medical system, Andover, MA). Full-volume acquisition over two heartbeats (for loop storage) was performed using ECG-gating over four cardiac cycles, during a quiet breath-hold if possible. Frame rate was maximized to allow quantification from RV-dedicated software and follow the current quantification guidelines (frame rate > 20 Hz)[12]. Care was taken to include the entire RV within the images. Digital 3D datasets were stored and analysed using RV-dedicated commercial software (4D RV Function 2.0, TomTec Imaging Systems GmbH, DE). This software allowed semi-automatic delineation of the RV endocardium, which was then automatically tracked across the cardiac cycle, and resulted in a sequence of 3D triangulated meshes with point-to-point correspondences (i.e. each vertex is labelled similarly across the cycle and subjects). It also provided an estimation of the RV end-diastolic and end-systolic volumes, ejection fraction, and wall-specific peak strain.

Preprint version accepted to appear in European Heart Journal Cardiovascular Imaging.
Final version of this paper available at https://academic.oup.com/ehjcimaging

An example of adequate RV tracking is illustrated for a patient with a primum atrial septal defect in Figure 1.

3D deformation analysis

The commercial software also allows exporting the RV surface meshes tracked along the cardiac cycle for external post-processing. For each subject, we computed deformation locally (at each point of the RV endocardial surface), and regionally/globally (average over a given segment or the whole ventricle) using VTK (v7.10, Kitware, New York, US), similar to our previous work[15]. Our results focus on end-systolic strain values. Circumferential and longitudinal strain computations were based on the *nominal strain* ---the relative change of length from end-diastole, also referred to as *engineering strain* or *Cauchy strain*--- along these directions, within a 5mm neighbourhood. Nonetheless, the computation of the circumferential and longitudinal directions may introduce additional variability due to the lack of consensus in their 3D definition, in particular for the RV. As a complement, we also provide area strain, computed as the relative change of area from end-diastole for each triangle of the RV surface mesh. This definition does not involve the circumferential and longitudinal directions and therefore does not suffer the above-mentioned limitation. Besides, under the hypothesis of an incompressible myocardium, it represents a relevant surrogate for radial deformation, which cannot be accessed otherwise as only endocardial surfaces are available.

Preprint version accepted to appear in European Heart Journal Cardiovascular Imaging.
Final version of this paper available at https://academic.oup.com/ehjcimaging

3D shape analysis

We also estimated the curvature at each point of the RV, at end-diastole. We used the "mean curvature" definition, which stands for the average of principal curvatures, as used in previous studies[6,7]. Positive/negative curvature means that the surface locally bends towards/ away from the centre of the RV. This 3D curvature analysis provides a detailed quantitative evaluation of RV remodelling patterns over the whole endocardial surface, which is not accessible with conventional 2D measurements and global values such as volumes. Computations used the Computational Geometry Algorithms Library (CGAL 4.11, Inria, FR)[16], which relies on smooth differential geometry calculations and approximates the local surface with a quadric, over a circular neighbourhood of 10mm (2 rings of nearest neighbours around the point of interest). This neighbourhood size was chosen a priori, small enough to prevent over smoothing of the data and reflect local changes, but not too small to be robust to local noisy surface variations.

Local/regional/global analysis

Spatial correspondences between the subjects' 3D deformation and curvature data were obtained by using the labels attached to the mesh vertices by the commercial software, which were consistent across the cycle and subjects. Temporal correspondences were achieved by normalizing these data according to the onset and end of the cardiac

Preprint version accepted to appear in European Heart Journal Cardiovascular Imaging.
Final version of this paper available at https://academic.oup.com/ehjcimaging

cycle. These steps are compulsory to compare the local 3D deformation and curvature data across subjects.

In addition, the RV was labelled according to the regions defined in Haddad *et al*.[17], and regional/global values were obtained by averaging the local deformation and curvature values over these regions / the whole ventricle.

These computations were carried out in Matlab (v.R2011a, MathWorks, Natick, US, USA).

Statistical analysis

Data were summarized as mean ± standard deviation for continuous variables with normal distribution; median [95% confidence interval] for other continuous variables and number of subjects (%) for categorical variables. Inter-group differences were assessed by the Student t-test for normally distributed variables, or the Mann-Whitney U-test otherwise, and categorical variables were compared using Fisher's exact test. Bonferroni correction was used for multiple comparisons (ANOVA). Correlation coefficients were calculated between the regional curvature and deformation values. These analyses were performed using MedCalc 19.1 (MedCalc Software, Mariakerke, BE).

Inter-group differences in the local curvature and deformation data were assessed by the Hotelling's T-Square test statistic[18] using Matlab (v.R2011a, MathWorks, Natick, US, USA), which returned a p-value at each point of the RV, low p-value indicating high differences. These values were

Preprint version accepted to appear in European Heart Journal Cardiovascular Imaging.
Final version of this paper available at https://academic.oup.com/ehjcimaging

visualized on the average shape representative of each subgroup, obtained by standard computational anatomy tools (generalized Procrustes analysis), and displayed in a customized logarithmic colour-scale to better visualize significantly different regions.

In all analyses, statistical significance was defined as a p-value < 0.05.

RESULTS

General characteristics of the population

Our study included 110 patients: 28 patients after TOF repair, 27 ASD patients and 55 controls. Controls and patients were matched for sex and age. General characteristics of the study groups are presented in Table 1.

Among TOF patients, 7 had initially a Blalock-Taussig shunt (25%) and all underwent a complete repair during childhood (the latest repair occurred at 15 years old in one patient). TOF repair included a trans-annular patch in 23 patients (82.1%). All TOF patients had significant pulmonary regurgitation, 3 of them had already had pulmonary valve replacement (but still suffered from significant pulmonary regurgitation).

Among ASD patients, all patients had significant defects with 2D echocardiographic evidence of RV chronic volume loading. Twenty-three had secundum ASD (85.2%), 3 had a sinus venosus defect (11.1%) and 1 had a primum ASD (3.7%). Seven suffered from embolic ischemic stroke

Preprint version accepted to appear in European Heart Journal Cardiovascular Imaging.
Final version of this paper available at https://academic.oup.com/ehjcimaging

(25.9%) and 5 (18.5%) presented paroxysmal supra-ventricular tachycardia, but all patients were in sinus rhythm at the time of the study.

Two-dimensional echocardiographic measurements are summarized in Table 2. All patients had a dilated right ventricle. RV diameter was not statistically different between ASD and TOF patients.

Compared to ASD patients, TOF patients had a more hypertrophic right ventricle ($p<0.001$) but reduced longitudinal contraction at the tricuspid annulus (reduced TAPSE ($p<0.001$) and tricuspid valve s' ($p=0.006$)).

3D strain analysis

Results from the analysis of 3D regional and global deformation are presented in Table 3. ASD and TOF patients have larger volumes than controls ($p<0.001$), while TOF patients also have a reduced RV EF ($p<0.001$).

Strain tends to be higher in ASD patients compared to controls, but these differences were not significant regarding RV area, longitudinal and circumferential strains, at the global RV level and at the regional level.

In contrast, many differences were observed between TOF patients and controls. RV area and circumferential strains were lower in TOF patients, especially in the RV free wall and in the trabecular / apical septum (Figures 2 and 3). Longitudinal strain was also significantly decreased in TOF patients, at slightly different locations (Figure 3). The inlet septum and superior part of the free wall were preserved compared

Preprint version accepted to appear in European Heart Journal Cardiovascular Imaging.
Final version of this paper available at https://academic.oup.com/ehjcimaging

to healthy controls. The ratio circumferential / longitudinal strain in TOF patients did not significantly differ from controls, which confirms that the extent of strain decrease was similar for longitudinal and circumferential strain.

TOF and ASD patients significantly differed regarding all variables, in almost all segments. Area strain mainly differed in the RV free wall, but the inlet and posterior septum looked preserved (Figure 2 and 3). Longitudinal and circumferential strain mostly differed in the RV free wall and the apical septum.

3D curvature analysis

Figure 4 summarizes curvature differences between ASD and TOF patients and controls. ASD patients and controls significantly differed in the extreme borders of the RV, the apex, and the septum. Differences were also marked between TOF and controls, mainly at the septal level, and the lateral and inferior walls. They were less visible between TOF and ASD patients, except in the operated RV outflow tract. No correlation was found between the regional curvature and strain values.

DISCUSSION

RV chronic volume loading results in different adaptations depending on the underlying congenital heart disease. Our analysis examined differences in the 3D patterns of RV shape and deformation, and therefore

Preprint version accepted to appear in European Heart Journal Cardiovascular Imaging.
Final version of this paper available at https://academic.oup.com/ehjcimaging

provides finer insights into the differences in ASD and TOF patients compared to controls.

3D RV shape differences

Assessing RV shape differences locally and in 3D is challenging. Indeed, there is no standard to appreciate RV shape, especially using 3D echocardiography. RV shape has been previously described using curvature from 3D-echocardiography in healthy volunteers[19], pulmonary arterial hypertension[6] and LVAD patients[7].

We had previously hypothesized that RV shape would be affected differently depending on the underlying pathology and thus, that a detailed assessment of RV shape would reveal differences between TOF and ASD patients. It was not the case. Despite coming from different sources (the right atrium or the pulmonary valve), the chronic volume loading affects the RV shape similarly in both subgroups. Even when quantifying an advanced descriptor such as curvature, locally and in 3D, no significant differences between ASD and TOF patients were observed.

However, patients with chronic volume loading were very different from controls and had lower curvature and more dilated shapes. In TOF patients, the infundibulum is significantly less curved than in ASD patients (Figure 4), which was expected given the history of ventricular septal defect and trans-annular patch in more than 80% of TOF patients during surgical correction. The detrimental role of the RV outflow tract akinesia has already been demonstered[20] regarding the decreased RV systolic

Preprint version accepted to appear in European Heart Journal Cardiovascular Imaging.
Final version of this paper available at https://academic.oup.com/ehjcimaging

function but also the onset of ventricular arrythmias[21]. Due to limited magnetic resonance data, we could not relate infundibular curvature data to the extent of the akinetic RV outflow tract area.

Other studies tried to assess RV shape in TOF patients: Zhong et al.[22] used cardiac magnetic resonance data but failed to demonstrate any difference at the RV outflow tract level between TOF patients and controls. In contrast, a recent 3D magnetic resonance study pointed out curvature differences at the RV outflow tract level between TOF and control patients but no difference in this area between TOF patients with or without trans-annular patch[23]. Our study goes further by jointly assessing RV shape and strain in TOF patients, and in 3D and locally, using 3D echocardiography. However, our cohort of patients was too limited to distinguish patterns depending on the type of repair, with more than 80% patients having history of trans-annular patch.

Previous authors implied that mechanical wall stress was inversely proportional to the local RV curvature[2]. The characterization of RV shape with local 3D curvature indirectly reflects the effects of chronic volume loading and allows better understanding of RV remodelling. While marked differences in strain data were observed in the trabecular septum, no significant difference in curvature was observed between TOF and ASD patients, indicating that RV shape may carry independent information. Therefore, for the assessment of TOF patients, RV shape and deformation could provide complementary insights into disease, and their potential for prognosis should be confirmed on larger cohort.

Preprint version accepted to appear in European Heart Journal Cardiovascular Imaging.
Final version of this paper available at https://academic.oup.com/ehjcimaging

3D RV strain differences

RV deformation differed between ASD and TOF patients. This difference has already been suggested in children but only focusing on 2D analysis and longitudinal strain[2]. While ASD patients and controls had similar circumferential and longitudinal strain, TOF patients had markedly reduced area, longitudinal and circumferential strains. These observations agree with other echocardiographic data: 3D ejection fraction, TAPSE and tricuspid valve s' are all reduced in TOF patients under the influence of the reduced global RV deformation.

In contrast, chronic volume loading in ASD seems to slightly increase RV deformation, as previously reported[24, 25]. Our study demonstrates that both longitudinal and circumferential strains are preserved in ASD (physiological response probably related to the increased wall shear stress[26]), contrary to what is observed for TOF patients. However, only little is known about RV remodelling after ASD closure. Some authors suggested that RV function after ASD closure (either surgical or interventional closure) declines compared to the pre-intervention assessment[25,27]. Regional differences in patients with open ASD have also been described[28] using 2D echocardiography, with increased apical longitudinal strain that also correlates with volume load severity. However, in our study, no significant difference was observed between ASD and controls, only a trend toward both higher area, longitudinal and circumferential strain.

Preprint version accepted to appear in European Heart Journal Cardiovascular Imaging.
Final version of this paper available at https://academic.oup.com/ehjcimaging

RV characteristics in TOF patients

ASD patients showed a better RV remodelling pattern than TOF patients. TOF patients had a more hypertrophic RV (significantly higher wall thickness) but reduced systolic function and strain despite very good clinical adaptation (no difference in NYHA class between TOF and ASD patients). The reduced RV strain in TOF patients might be explained by several factors: an abnormal development, the prior pre-op RV pressure overload and RV hypertrophy (observed in our cohort), a large ventriculotomy, the influence of myocardial damage related to prolonged cyanosis and surgery and the advanced age of our TOF cohort.

RV dyssynchrony may also affect the strain pattern across the cycle and therefore the end-systolic values, as reported on 2D echocardiographic data[29]. In our population, TOF patients had significantly longer QRS duration, which has been shown to impact RV function more than PR[30].

Regarding the impact of surgery at the regional level, differences in RV strain between TOF patients and the other subgroups was not only observed within the infundibular area, but also and predominantly in the RV free wall, suggesting a global remodelling.

Differential regional effects of RV chronic volume loading have been observed in TOF. During the last decade, authors emphasized the importance of regional differences within the RV of TOF patients[31], as also suggested by our study, with a variable adaptive response to isolated

Preprint version accepted to appear in European Heart Journal Cardiovascular Imaging.
Final version of this paper available at https://academic.oup.com/ehjcimaging

chronic volume loading as opposed to combined pressure/volume overload. The role of the apex has been previously underlined, with a loss of function in TOF patients[2]. In our study, the use of 3D echocardiography allows analysing more precisely differences in TOF patients (regionally and locally).

Limitations

Curvature assessment was performed on end-diastolic shapes, to avoid mixing the effect of systolic contraction on RV shape. However, analysing the RV shape throughout the whole cardiac cycle might provide complementary insights, especially in TOF patients, knowing the role of dyssynchrony in those[32].

Apart from the detailed area strain patterns, we also reported regional and global area strain values, meaning that area strain was averaged over a given region or the whole RV. We did not consider changes in the area of the RV regions or the whole RV for the sake of clarity, although this slightly different computation should lead to similar conclusions.

3D RV study was feasible in all of our patients, however this method is hardly applicable to patients with poor acoustic windows. Our study was monocentric and suffers from a lack of power given the relatively small cohort of patients. Current guidelines[33] do not recommend routine assessment of 3D RV volumes and deformation given the paucity of normal data in congenital heart disease patients. Thus, future work should

Preprint version accepted to appear in European Heart Journal Cardiovascular Imaging.
Final version of this paper available at https://academic.oup.com/ehjcimaging

aim at increasing the cohorts of both healthy controls and CHD patients from multicentre acquisitions, further analysed using the same methodology. Larger amount of cases in each subgroup would also allow examining the complex relationship between RV size or shape and deformation descriptors. Investigating the relationship between RV pressure and strain would require a different cohort of patients, as we carefully excluded patients with residual pulmonary stenosis.

Finally, the current version of the commercial software only allowed us to analyse a single layer across the RV wall. Processing different layers may help investigate complementary shape and deformation characteristics across the wall.

CONCLUSION

With 3D assessment up to each point of the RV endocardial surface, our study demonstrates differences in RV function between ASD patients (preserved deformation) and TOF patients (reduced deformation), despite comparable shape remodelling. Left-to-right atrial shunt and pulmonary regurgitation are responsible for different types of RV remodelling, probably related to the underlying myocardial substrate in TOF patients.

ACKNOWLEDGMENTS

The authors would like to thank Shuman Jia and Come Le Breton (Inria) for their help with the CGAL software.

Preprint version accepted to appear in European Heart Journal Cardiovascular Imaging.
Final version of this paper available at https://academic.oup.com/ehjcimaging

Funding sources: This study was partly funded by a grant from the University hospital of Nice, France (AO2I-2013). The authors also acknowledge the partial support from the European Union 7th Framework Program (VP2HF FP7-2013-611823).

Preprint version accepted to appear in European Heart Journal Cardiovascular Imaging.
Final version of this paper available at https://academic.oup.com/ehjcimaging

REFERENCES

1. Mertens LL, Friedberg MK. Imaging the right ventricle--current state of the art. Nat Rev Cardiol 2010; 7:551-63.
2. Dragulescu A, Grosse-Wortmann L, Redington A, Friedberg MK, Mertens L. Differential effect of right ventricular dilatation on myocardial deformation in patients with atrial septal defects and patients after tetralogy of Fallot repair. Int J Cardiol 2013; 168:803-10.
3. Reddy S, Bernstein D. Molecular Mechanisms of Right Ventricular Failure. Circulation 2015; 132:1734-42.
4. Bouzas B, Kilner PJ, Gatzoulis MA. Pulmonary regurgitation: not a benign lesion. Eur Heart J 2005; 26:433-9.
5. Rashid I, Mahmood A, Ismail TF, O'Meagher S, Kutty S, Celermajer D, et al. Right ventricular systolic dysfunction but not dilatation correlates with prognostically significant reductions in exercise capacity in repaired Tetralogy of Fallot. Eur Heart J Cardiovasc Imaging 2019. *In Press.* doi: 10.1093/ehjci/jez245
6. Addetia K, Maffessanti F, Yamat M, Weinert L, Narang A, Freed BH, et al. Three-dimensional echocardiography-based analysis of right ventricular shape in pulmonary arterial hypertension. Eur Heart J Cardiovasc Imaging 2016; 17:564-75.
7. Addetia K, Uriel N, Maffessanti F, Sayer G, Adatya S, Kim GH, et al. 3D Morphological Changes in LV and RV During LVAD Ramp Studies. JACC Cardiovasc Imaging 2018; 11:159-169.
8. Silvestry FE, Cohen MS, Armsby LB, Burkule NJ, Fleishman CE, Hijazi ZM, et al. Guidelines for the Echocardiographic Assessment of Atrial Septal Defect and Patent Foramen Ovale: From the American Society of Echocardiography and Society for Cardiac Angiography and Interventions. J Am Soc Echocardiogr 2015; 28:910-58.
9. Li W, Davlouros PA, Kilner PJ, Pennell DJ, Gibson D, Henein MY, et al. Doppler-echocardiographic assessment of pulmonary regurgitation in

adults with repaired tetralogy of Fallot: comparison with cardiovascular magnetic resonance imaging. Am Heart J 2004; 147:165-72.

10. Renella P, Aboulhosn J, Lohan DG, Jonnala P, Finn JP, Satou GM, et al. Two-dimensional and Doppler echocardiography reliably predict severe pulmonary regurgitation as quantified by cardiac magnetic resonance. J Am Soc Echocardiogr 2010; 23:880-6.

11. Valente AM, Cook S, Festa P, Ko HH, Krishnamurthy R, Taylor AM, et al. Multimodality imaging guidelines for patients with repaired tetralogy of fallot: a report from the American Society of Echocardiography: developed in collaboration with the Society for Cardiovascular Magnetic Resonance and the Society for Pediatric Radiology. J Am Soc Echocardiogr 2014; 27:111-41.

12. Rudski LG, Lai WW, Afilalo J, Hua L, Handschumacher MD, Chandrasekaran K, et al. Guidelines for the Echocardiographic Assessment of the Right Heart in Adults: A Report from the American Society of Echocardiography. J Am Soc Echocardiogr 2010; 23:685-713.

13. Douglas PS, DeCara JM, Devereux RB, Duckworth S, Gardin JM, Jaber WA, et al. Echocardiographic Imaging in Clinical Trials: American Society of Echocardiography Standards for Echocardiography Core Laboratories. J Am Soc Echocardiogr 2009; 22:755-765.

14. Lang RM, Badano LP, Mor-Avi V, Afilalo J, Armstrong A, Ernande L, et al. Recommendations for cardiac chamber quantification by echocardiography in adults: an update from the American Society of Echocardiography and the European Association of Cardiovascular Imaging. Eur Heart J Cardiovasc Imaging 2015; 16:233-70.

15. Moceri P, Duchateau N, Baudouy D, Schouver ED, Leroy S, Squara F, et al. Three-dimensional right-ventricular regional deformation and survival in pulmonary hypertension. Eur Heart J Cardiovasc Imaging 2018; 19:450-458.

14. Addetia K, Maffessanti F, Yamat M, Weinert L, Narang A, Freed BH, et al. Three-dimensional echocardiography-based analysis of right ventricular

shape in pulmonary arterial hypertension. Eur Heart J Cardiovasc Imaging 2016; 17:564-75.

15. Addetia K, Uriel N, Maffessanti F, Sayer G, Adatya S, Kim GH, et al. 3D Morphological Changes in LV and RV During LVAD Ramp Studies. JACC Cardiovasc Imaging 2018; 11:159-169.

16. Board CE. CGAL 4.11, Computational Geometry Algorithms Library, http://www.cgal.org/. 2017.

17. Haddad F, Hunt SA, Rosenthal DN, Murphy DJ. Right ventricular function in cardiovascular disease, part I: Anatomy, physiology, aging, and functional assessment of the right ventricle. Circulation 2008; 117:1436-48.

18. Hotelling H. The generalization of Student's ratio. Annals of Mathematical Statistics 1931; 2:360-378.

19. Addetia K, Maffessanti F, Muraru D, Singh A, Surkova E, Mor-Avi V, et al. Morphologic Analysis of the Normal Right Ventricle Using Three-Dimensional Echocardiography-Derived Curvature Indices. J Am Soc Echocardiogr 2018; 31:614-623.

20. Davlouros PA, Kilner PJ, Hornung TS, Li W, Francis JM, Moon JC, et al. Right ventricular function in adults with repaired tetralogy of Fallot assessed with cardiovascular magnetic resonance imaging: detrimental role of right ventricular outflow aneurysms or akinesia and adverse right-to-left ventricular interaction. J Am Coll Cardiol 2002; 40:2044-52.

21. Bonello B, Kempny A, Uebing A, Li W, Kilner PJ, Diller GP, et al. Right atrial area and right ventricular outflow tract akinetic length predict sustained tachyarrhythmia in repaired tetralogy of Fallot. Int J Cardiol 2013; 168:3280–3286.

22. Zhong L, Gobeawan L, Su Y, Tan JL, Ghista D, Chua T, et al. Right ventricular regional wall curvedness and area strain in patients with repaired tetralogy of Fallot. Am J Physiol Heart Circ Physiol 2012; 302:H1306-16.

23. Zaidi SJ, Cossor W, Singh A, Maffesanti F, Kawaji K, Woo J, et al. Three-dimensional analysis of regional right ventricular shape and function in repaired tetralogy of Fallot using cardiovascular magnetic resonance. Clin Imaging 2018; 52:106-112.
24. Eyskens B, Ganame J, Claus P, Boshoff D, Gewillig M, Mertens L. Ultrasonic strain rate and strain imaging of the right ventricle in children before and after percutaneous closure of an atrial septal defect. J Am Soc Echocardiogr 2006; 19:994-1000.
25. Jategaonkar SR, Scholtz W, Butz T, Bogunovic N, Faber L, Horstkotte D. Two-dimensional strain and strain rate imaging of the right ventricle in adult patients before and after percutaneous closure of atrial septal defects. Eur J Echocardiogr 2009; 10:499-502.
26. Hayabuchi Y, Sakata M, Ohnishi T, Kagami S. A novel bilayer approach to ventricular septal deformation analysis by speckle tracking imaging in children with right ventricular overload. J Am Soc Echocardiogr 2011; 24:1205-12.
27. Ko HK, Yu JJ, Cho EK, Kang SY, Seo CD, Baek JS, et al. Segmental Analysis of Right Ventricular Longitudinal Deformation in Children before and after Percutaneous Closure of Atrial Septal Defect. J Cardiovasc Ultrasound 2014; 22:182-8.
28. Van De Bruaene A, Buys R, Vanhees L, Delcroix M, Voigt JU, Budts W. Regional right ventricular deformation in patients with open and closed atrial septal defect. Eur J Echocardiogr 2010; 12:206-213.
29. Hui W, Slorach C, Dragulescu A, Mertens L, Bijnens B, Friedberg MK. Mechanisms of right ventricular electromechanical dyssynchrony and mechanical inefficiency in children after repair of tetralogy of fallot. Circ Cardiovasc Imaging 2014; 7:610-8.
30. Lumens J, Fan CS, Walmsley J, Yim D, Manlhiot C, Dragulescu A, et al. Relative impact of right ventricular electromechanical dyssynchrony versus pulmonary regurgitation on right ventricular dysfunction and

exercise intolerance in patients after repair of tetralogy of Fallot. J Am Heart Assoc 2019; 8:e010903.

31. Bodhey NK, Beerbaum P, Sarikouch S, Kropf S, Lange P, Berger F, et al. Functional analysis of the components of the right ventricle in the setting of tetralogy of Fallot. Circ Cardiovasc Imaging 2008; 1:141-7.

32. Friedberg MK, Fernandes FP, Roche SL, Slorach C, Grosse-Wortmann L, Manlhiot C, et al. Relation of right ventricular mechanics to exercise tolerance in children after tetralogy of Fallot repair. Am Heart J 2013; 165:551-7.

33. Simpson J, Lopez L, Acar P, Friedberg MK, Khoo NS, Ko HH, et al. Three-dimensional Echocardiography in Congenital Heart Disease: An Expert Consensus Document from the European Association of Cardiovascular Imaging and the American Society of Echocardiography. J Am Soc Echocardiogr 2017; 30:1-27.

Preprint version accepted to appear in European Heart Journal Cardiovascular Imaging.
Final version of this paper available at https://academic.oup.com/ehjcimaging

FIGURE TITLES AND LEGENDS

Figure 1: Example of RV endocardial tracking in an ASD patient.

Top: Identification of LV/RV landmarks as suggested by the software. Middle: verification of the automatic RV endocardial tracking. Bottom: output values (RV volumes and ejection fraction, and 3D RV mesh to be exported).

Figure 2: Area strain represented over the average RV shape for each subgroup.

Top two rows: RV septum; bottom two rows: RV free wall. Rows respectively represent the median area strain pattern, and the corresponding statistical differences between subgroups (controls vs. ASD and TOF patients, as well as ASD vs. TOF patients). The customized colour-scale allows better visualizing the statistically significant differences: p-values <0.05 are red – orange – yellow and green, whereas blue indicates no significant difference between the studied groups. This figure confirms at a finer level (local comparisons) the differences in area strain observed regionally in Table 3, especially in TOF patients against controls and ASD patients.

Figure 3: Circumferential and longitudinal strains represented over the average RV shape for each subgroup.

Preprint version accepted to appear in European Heart Journal Cardiovascular Imaging.
Final version of this paper available at https://academic.oup.com/ehjcimaging

Display similar to Figure 2. The figure illustrates the lower circumferential strain in TOF patients, especially at the apex, and major differences in longitudinal strain within the trabecular septum, the apex and the lateral wall.

Figure 4: RV curvature represented over the average RV shape for each subgroup.

Display similar to Figure 2. Statistically significant differences are observed within the septum between RV chronic volume loading patients and controls, whereas almost no difference is visible between TOF and ASD patients, except within the right ventricular outflow tract.

Preprint version accepted to appear in European Heart Journal Cardiovascular Imaging.
Final version of this paper available at https://academic.oup.com/ehjcimaging

TABLES

Table 1: Main characteristics of the study groups

		Controls n=55	ASD n=27	Tetralogy of Fallot n=28	p-value
Age, years		33.0[28.0-36.0]	30.0[19.0-42.1]	31.0[24.4-34.0]	0.42
Female sex, n (%)		10 (47.6%)	11 (73.3%)	9 (60%)	0.46
Height, cm		166.3±7.6	167.2±11.2	166.2±11.8	0.71
Weight, kg		69.3±14.1	70.5±17.1	66.2±18.4	0.81
NYHA class, n(%)	**I or II**	-	22 (81.5%)	23 (82.1%)	0.96
	III	-	5 (18.5%)	5 (17.9%)	0.95
Heart rate, bpm		68.3±12.4	76.1±13.4	79.3±15.2	0.73
BNP, ng/mL		-	72.2[45.9-81.0]	85.0[49.3-96.8]	0.39
QRS duration, ms		-	104.0[87.1-108.9]	140.0[121.3-167.2]	**0.0006**
Frame rate, Hz		26.0[24.0-28.0]	23.0[21.6-26.0]	25.0[22.0-26.0]	0.53

ASD, atrial septal defect; BNP, brain natriuretic peptide; NYHA, New York Heart Association; PAH, pulmonary arterial hypertension

Preprint version accepted to appear in European Heart Journal Cardiovascular Imaging.
Final version of this paper available at https://academic.oup.com/ehjcimaging

Table 2: Echocardiographic characteristics of the study groups

	ASD n=27	Tetralogy of Fallot n=28	p-value
RV diameter, mm	43.0[40.2-48.0]	45.0[42.7-49.3]	0.35
RV wall thickness, mm	5.0[4.0-5.5]	8.0[6.7-8.3]	**<0.001**
TAPSE, mm	28.0[24.1-30.9]	19.0[18.0-20.0]	**<0.001**
TV s', cm/s	14.9±3.4	10.8±3.3	**0.006**
LV EF, %	60.6±5.6	60.8±8.3	0.96

ASD, atrial septal defect; EF, ejection fraction; LV, left ventricular; RV, right ventricular; TAPSE, tricuspid annular plane systolic excursion; TV s', tricuspid annular peak systolic velocity.

Preprint version accepted to appear in European Heart Journal Cardiovascular Imaging.
Final version of this paper available at https://academic.oup.com/ehjcimaging

Table 3: 3D echocardiographic and strain data

	Controls n=55	ASD n=27	Tetralogy of Fallot n=28	p-value
RV EDV, mL	63.0[56.8-67.2]	150.0[121.9-163.0]	163.0[116.1-183.6]	**<0.001**
RV EF, %	56.0[52.9-57.0]	56.0[52.9-59.1]	48.0[43.0-50.6]	**<0.001**
RV Area strain, %				
Global	-31.5±5.8	-34.1±7.9	-24.8±5.7	**<0.001**
Anterior wall	-27.9±8.6	-31.5±8.6	-21.6±7.5	**<0.001**
Inferior wall	-36.6±8.2	-39.4±8.5	-29.3±9.3	**<0.001**
Lateral wall	-41.2±6.7	-40.5±8.8	-28.1±6.7	**<0.001**
RVOT anterior	-21.8±6.8	-25.3±7.0	-18.3±6.2	**0.001**
Infundibular septum	-27.6±8.5	-30.9±8.2	-23.2±6.1	**0.002**
Membranous septum	-22.7±8.4	-25.7±10.4	-19.3±6.4	**0.02**
Inlet septum	-26.8±10.9	-31.4±11.3	-26.3±7.2	0.11
Trabecular septum	-25.4±8.2	-29.7±7.9	-20.4±6.3	**<0.001**
RV Circumferential strain, %				
Global	-18.8±3.7	-20.5±5.3	-15.2±3.9	**<0.001**
Anterior wall	-18.7±8.0	-20.9±6.6	-14.1±7.7	**0.004**
Inferior wall	-19.8±6.0	-22.1±6.2	-16.5±6.6	**0.004**
Lateral wall	-27.8±5.2	-27.4±6.7	-19.1±4.9	**<0.001**
RVOT anterior	-10.7±5.3	-12.5±5.1	-10.3±4.8	0.23
Infundibular septum	-16.5±4.7	-19.2±5.0	-16.3±5.0	**0.04**
Membranous septum	-12.5±4.5	-15.4±6.0	-11.8±3.8	**0.01**
Inlet septum	-15.5±6.1	-17.6±7.1	-16.0±6.0	0.36
Trabecular septum	-13.6±5.6	-15.9±7.0	-10.6±4.6	**0.003**
RV Longitudinal strain, %				
Global	-14.2±4.6	-16.0±5.4	-10.3±3.0	**<0.001**
Anterior wall	-10.7±5.3	-12.9±5.5	-8.0±2.9	**0.001**
Inferior wall	-19.3±6.7	-21.1±5.7	-14.3±4.3	**<0.001**
Lateral wall	-15.5±4.6	-16.5±5.1	-10.0±3.1	**<0.001**
RVOT anterior	-12.0±6.1	-13.8±6.6	-8.7±3.6	**0.004**
Infundibular septum	-11.1±7.4	-12.2±8.8	-7.1±4.5	**0.02**
Membranous septum	-10.9±7.2	-11.7±8.0	-7.7±5.2	0.07
Inlet septum	-11.8±9.3	-15.2±8.7	-10.6±4.3	0.09
Trabecular septum	-12.9±5.4	-15.2±4.1	-10.3±3.6	**0.001**

ASD, atrial septal defect; EDV, end-diastolic volume; EF, ejection fraction; PH, pulmonary hypertension; RV, right ventricular; RVOT, right ventricular outflow tract.

Preprint version accepted to appear in European Heart Journal Cardiovascular Imaging.
Final version of this paper available at https://academic.oup.com/ehjcimaging

Figure 1

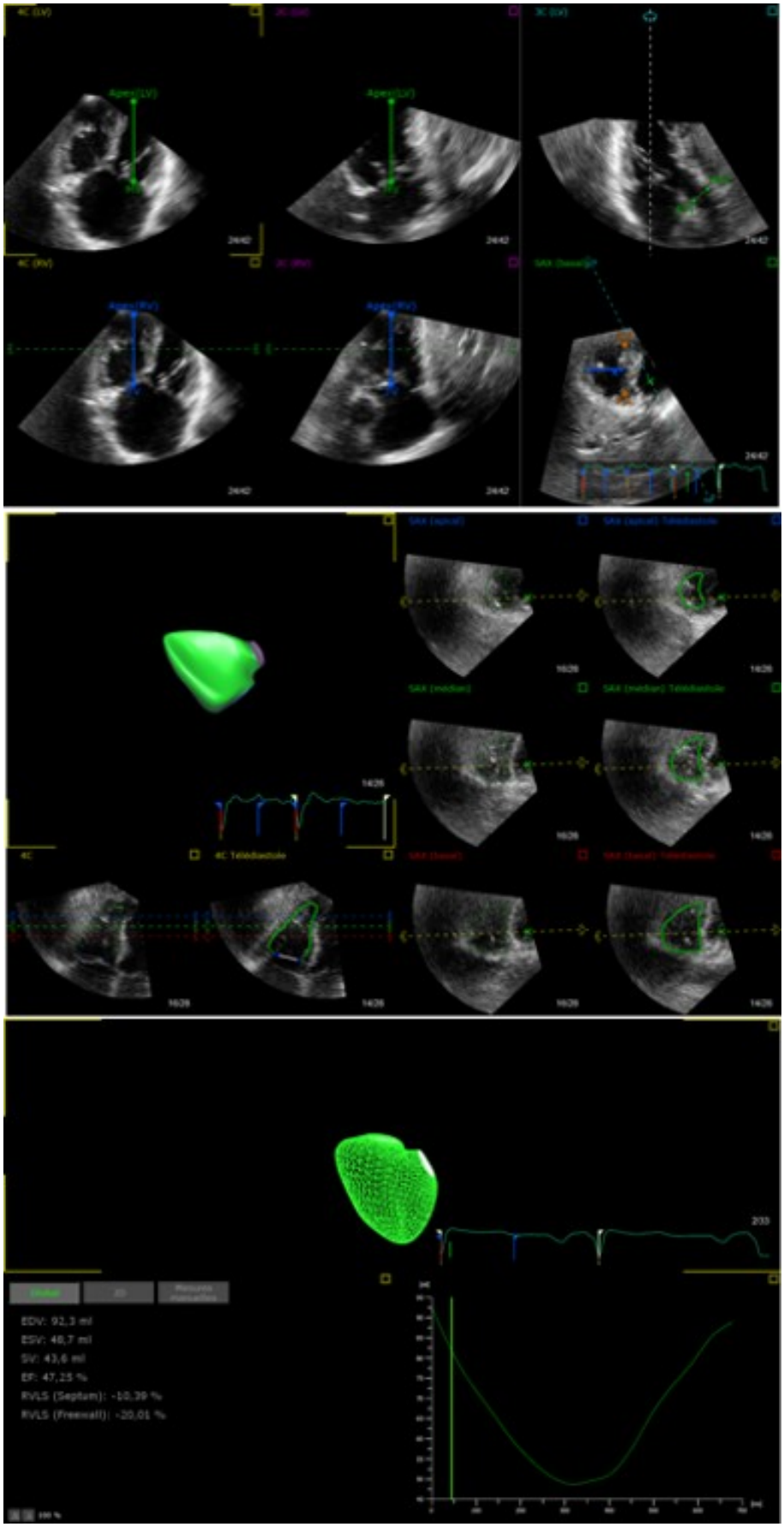

Preprint version accepted to appear in European Heart Journal Cardiovascular Imaging.
Final version of this paper available at https://academic.oup.com/ehjcimaging

Figure 2

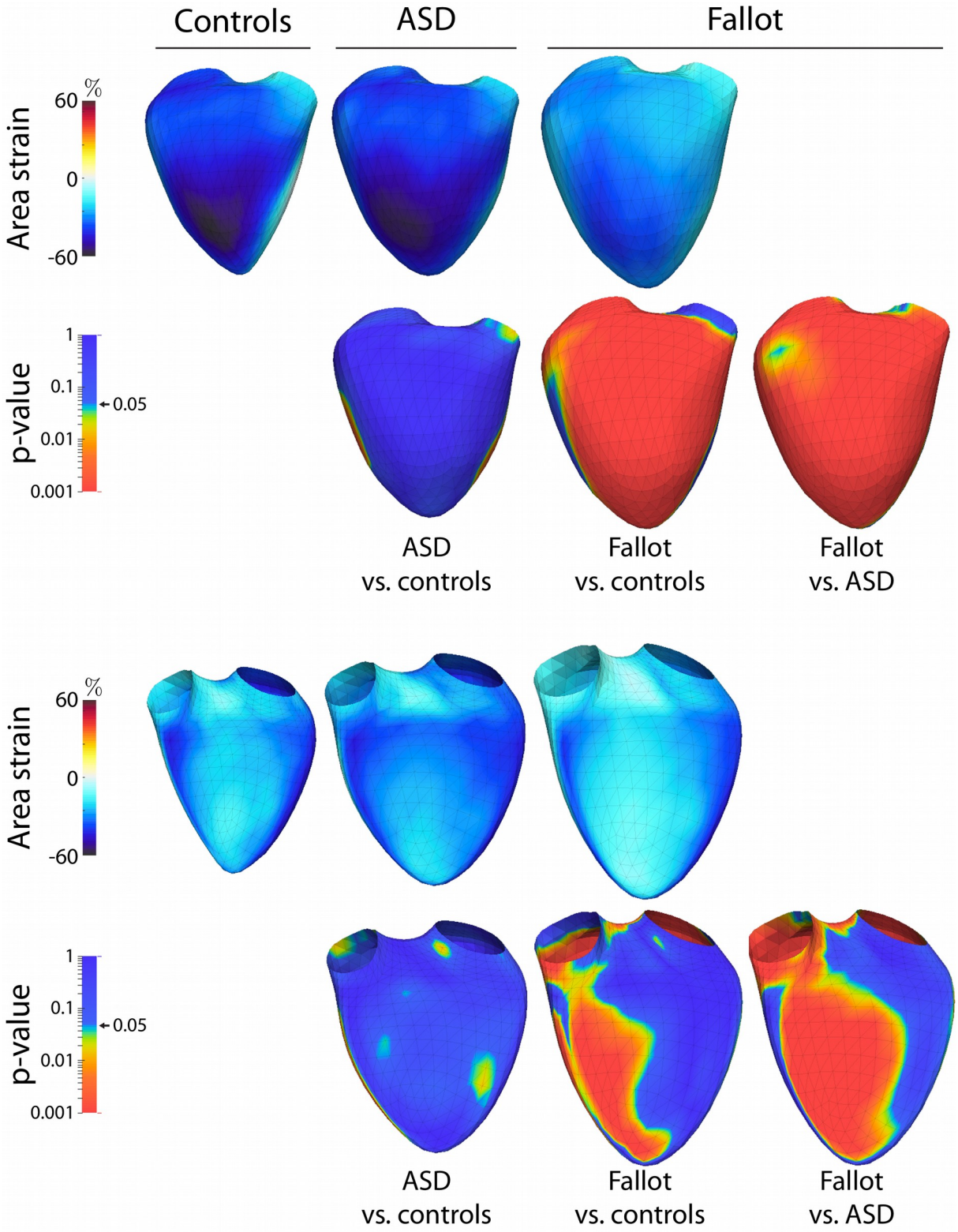

Preprint version accepted to appear in European Heart Journal Cardiovascular Imaging.
Final version of this paper available at https://academic.oup.com/ehjcimaging

Figure 3

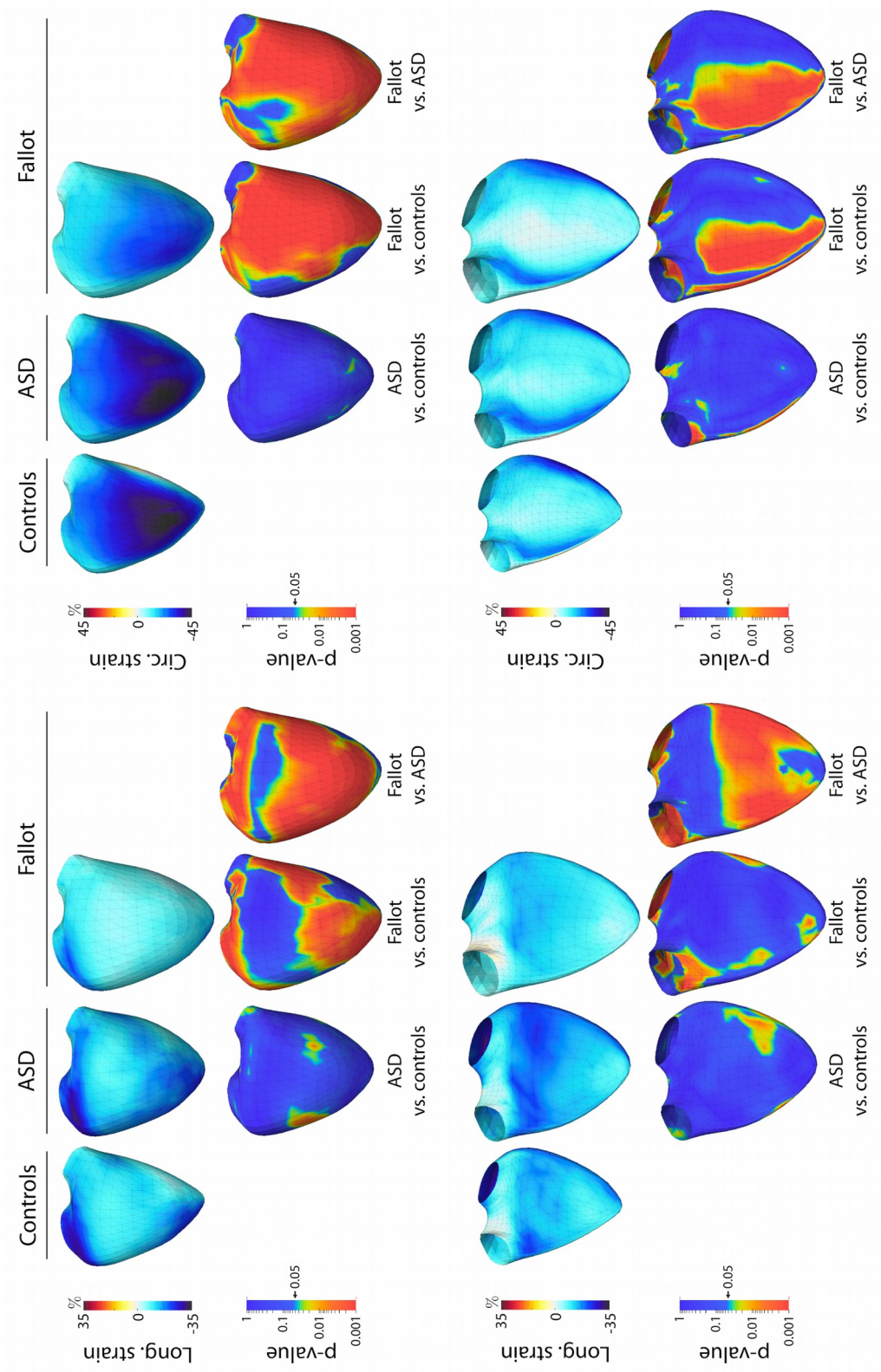

Preprint version accepted to appear in European Heart Journal Cardiovascular Imaging.
Final version of this paper available at https://academic.oup.com/ehjcimaging

Figure 4